Assessment of damping and nonlinearities on the roll responses of a VLCC in waves without forward speed

Claudio A. Rodríguez, Ieza S. Ramos, Paulo T. T. Esperança

Laboratory of Ocean Technology (LabOceano), Department of Naval Architecture and Ocean Engineering, Federal University of Rio de Janeiro, Brazil

claudiorc@oceanica.ufrj.br, iezaramos@poli.ufrj.br, ptarso@laboceano.coppe.ufrj.br

Mauro C. Oliveira, *Research and Development Center (CENPES) - Petróleo Brasileiro S.A., Rio de Janeiro, Brazil,* mauro@petrobras.com.br

ABSTRACT

Roll damping is one of the most important parameters for the direct stability assessment of the behavior of ships in waves. The complexity of the hydrodynamic phenomena involved in the roll motion makes its numerical prediction still an open issue and non-standardized task. Despite the greater improvements achieved in the recent years with computational fluid dynamics, for practical purposes, roll damping assessment is still highly dependent on model tests, particularly, roll decay tests in calm-water. The damping coefficients extrapolated from these tests are typically used as direct inputs in the numerical simulations of ship responses in waves.

Based on the results of an experimental test campaign with a VLCC hull, the present study evidences that the measured roll responses in waves can be significantly different from those predicted by numerical simulations that rely on roll decay damping coefficients. Linear frequency- and nonlinear time- domain numerical approaches have been adopted in the simulations. Based on the frequency domain linear model, an external viscous roll damping coefficient has been estimated for each (regular and irregular wave) test condition using the experimental roll response as reference. The analyses of the estimated roll damping coefficients from experimental data indicate that in waves, damping is stronger than in decay tests (in calm-water). On the numerical side, the effect of nonlinearities in hydrostatic and Froude-Krylov actions has been also investigated. It was concluded that, at least for the VLCC, those nonlinearities are less important than the accurate assessment of roll damping in the numerical simulation of roll responses in waves.

Keywords: *viscous damping, nonlinearities, SGISC, direct stability assessment.*

1. INTRODUCTION

In the context of the second-generation intact stability criteria (SGISC) being developed at the International Maritime Organization (IMO), direct stability assessment can be performed either by model tests or numerical simulations. In the latter case, reliable estimation of the probability of stability failure requires simulation of a sufficiently large number of stability failures for the relevant ships and loading conditions, considering as much relevant physics as possible in the most accurate way.

Since most of the stability failures addressed by the IMO SGISC directly involve the roll motion, roll damping naturally appears as a key factor for the numerical simulations of the ship responses in waves, especially when resonant behaviors take place. In the recent years, this topic has attracted renewed attention as evidenced by the number of papers concerning this issue in the last STAB 2018 and ISSW2019. Ikeda (2018) presented a historical review of his prediction method and stressed the need for further developments using, for instance, CFD tools. Smith (2018) explored and compared various typical methods of calculation of roll damping values from empirical data. Oliva-Remola *et al.* (2018) analyzed the influence of different experimental techniques for roll decay tests with a model of a trawler fishing vessel. Wassermann *et al.*

(2018), Hashimoto *et al.* (2019) and Oliveira *et al.* (2019) have also investigated the ship roll damping based on roll decay motions, using CFD and/or EFD. Katayama et al. (2019) proposed a rational short-term prediction method considering nonlinearity in roll damping and restoring moments. Oliva-Remola and Pérez-Rojas (2019) presented an approach for the assessment of uncertainty of roll decay tests and emphasized the difficulties in the determination of uncertainties associated to nonlinear damping coefficients. A more detailed review of the published works related to roll damping in STAB and ISSW conferences can be found in Bačkalov *et al.* (2016) and Manderbacka *et al.* (2019).

Most of the above references are focused on decay and/or forced excited roll conditions. The damping coefficients obtained from those tests, which are typically performed in calm water, are assumed to be representative of the roll damping in waves. This hypothesis, however, may not be reliable, especially when moderate sea conditions are considered. Furthermore, discrepancies in numerical predictions are usually attributed to nonlinearities in damping and/or restoring actions.

Based on the results from an experimental test campaign of a typical very large crude carrier (VLCC) in beam regular and irregular waves, the present work analyzes the roll responses and the associated damping coefficients to each test condition. First, decay tests results are analyzed using different approaches for the determination of the damping coefficients. Then, using a hybrid (numerical-experimental) linearized procedure, roll damping coefficients are determined from the model tests responses in waves. Furthermore, the semi-empirical Ikeda's prediction method has been implemented to assess the quality of the prediction of roll damping coefficients for the VLCC hull. Finally, numerical simulations of roll motions have been performed in time domain to allow the comparison among decay tests coefficients, the wave response-based coefficients and the simplified Ikeda's coefficients. The influence of nonlinearities in hydrostatics and Froude-Krylov actions on the prediction of roll motions have been also investigated.

2. ROLL DAMPING FROM DECAY TESTS

The roll motion, ϕ, for free decay in calm-water can be expressed as:

$$(I_{xx} + A_{44})\ddot{\phi} + B_{44}(\dot{\phi}) + C_{44}\phi = 0 \quad (1)$$

where I_{xx} is the roll inertia, A_{44} and C_{44} are the roll added mass and hydrostatic restoring coefficients. $B_{44}(\dot{\phi})$ denotes the roll damping moment, which is typically modeled as:

$$B_{44}(\dot{\phi}) = B_1\dot{\phi} + B_2\left|\dot{\phi}\right|\dot{\phi} \quad (2)$$

This roll damping model introduces a nonlinearity in the roll motion equation and makes it more difficult to analyze. So, usually nonlinear damping is replaced by a certain linearized damping, i.e.:

$$B_{44}(\dot{\phi}) = B_e\dot{\phi} \quad (3)$$

where B_e represents the equivalent linear damping coefficient which, in general, depends on the amplitude and period of roll motion. However, for a given cycle of motion, B_e can be considered constant. For a generic periodic motion, B_e can be expressed in terms of B_1 and B_2 by equating the first terms of the Fourier series expansion of eq. (2) and eq. (3), so that:

$$B_e(\phi_a) = B_1 + \frac{16}{3T_k}\phi_a B_2 \quad (4)$$

where the roll amplitude is $\phi_a = (\phi_k + \phi_{k+1})/2$, ϕ_k and ϕ_{k+1} denote two successive peaks in the roll decay motion, and T_k is the roll period. The damping coefficient B_e (or B_1 and B_2) can be obtained from analyses of roll decay time records. The most common methods are the logarithmic decrement method and the Froude energy method. A more detailed description and discussion on various other methods for roll decay analyses can be found in Spouge (1988).

3. ROLL DAMPING FROM WAVE TESTS

Based on the experimental ship responses in waves and a numerical model for the simulations of roll responses in waves, an external roll damping coefficient can be determined in the calibration process of the numerical roll response.

For the sake of simplicity, a linear frequency-domain numerical model was adopted for the uncouple roll motion equation in waves:

$$(I_{xx} + A_{44})\ddot{\phi} + B_{44}\dot{\phi} + C_{44}\phi = M_{\phi}(t) \quad (5)$$

where $M_\phi(t)$ represents the wave exciting moment in roll. In the calibration process, the roll damping coefficient was assumed linear and was subdivided in a potential (radiation) part plus a viscous contribution. The potential part was assumed frequency-dependent while the viscous contribution was allowed to change also with the incident wave height.

The calibration criterion for the regular wave tests is based on the mean amplitude of the roll response, which can be expressed as:

$$\hat{\phi}(\omega) = \frac{\hat{M}_{\phi}(\omega)}{-\omega^2\left[I_{xx} + A_{44}(\omega)\right] + i\omega B_{44}(\omega) + C_{44}} \quad (6)$$

where $\hat{\phi}$ and $\hat{M}_\phi$ are the complex amplitudes of the roll response and the excitation moment, $i = \sqrt{-1}$. The hydrodynamic potential coefficients and moments can be obtained using, for instance, WAMIT® or ANSYS-AQWA™. The response amplitude operator (RAO) of the motion relative to the incident wave can be defined by:

$$RAO_{\phi}(\omega) = \frac{\phi_a(\omega)}{\zeta_a(\omega)} \quad (7)$$

where $\zeta_a(\omega)$ is the amplitude of the incident wave and ϕ_a is the amplitude of the roll response.

For the irregular waves conditions the area under the roll response spectrum was used as calibration criterion of the numerical simulations of roll motion. The roll response spectrum can be obtained using the spectral approach, so that:

$$S_{\phi}(\omega) = \left|RAO_{\phi}(\omega)\right|^2 \cdot S_{\zeta}(\omega) \quad (8)$$

where $S_\zeta(\omega)$ and $S_\phi(\omega)$ denote the power spectral densities of the incident sea (wave spectrum) and the roll response (motion spectrum), respectively. The significant motion amplitude, $\phi_{1/3}$, is given by:

$$\phi_{1/3} = 2\sqrt{m_{0\phi}} \quad (9)$$

where $m_{0\phi}$ is the area under the roll response spectrum.

Further details on the determination of roll damping coefficients using the hybrid procedure can be found in Rodríguez *et al.* (2019).

4. ROLL DAMPING FROM IKEDA'S METHOD

A semi-empirical method for roll damping prediction of ships was proposed originally by Ikeda as described in Himeno (1981). The method assumes that the roll damping moment (B_{t4}) can be separated into components. Each one is computed independently and associated to skin friction (B_F), eddy shedding (B_E), hull lift (B_L), free-surface waves (B_W), and bilge keel effects. The bilge keel effect was subdivided in three components: B_{BKN} due to the normal force on the bilge keels themselves, B_{BKH} due to the pressure change on the hull when bilge keels are installed, i.e., the interaction between hull and bilge keels, and B_{BKW} due to the waves associated to the presence of bilge keels. Therefore:

$$B_{t4} = B_F + B_E + B_L + B_W + B_{BKN} + B_{BKH} + B_{BKW} \quad (10)$$

More recently, Kawahara *et al.* (2012) presented a simplified method of predicting roll damping following Ikeda's method. This simplified method requires only some main parameters of the ship instead of the detailed geometry of the ship cross sections (required by the original Ikeda's method). Once each of the components in eq. (10) is estimated, the total damping moment is presented as a function of the roll amplitude and the coefficients B_1 and B_2 obtained using eq. (4).

5. NUMERICAL MODEL FOR DIRECT STABILITY ASSESSMENT

The numerical model for the prediction of roll motions in time domain consists of two stages. In the first stage, a frequency domain approach based on 3D panel method is used to compute the linear radiation/diffraction forces as well as the response amplitude operators for the six degrees of freedom of the vessel. In the second stage, the equations of motions are solved in time-domain using either the linear or a nonlinear approach in the six-degrees of freedom.

For the linear approach, the radiation/diffraction forces come directly from the first stage and hydrostatics and Froude-Krylov forces are computed considering only the mean-wetted surface of the vessel. Linear external damping and/or hydrostatic

coefficients (associated for instance to linear mooring forces) can be introduced in any of the degrees of freedom.

For the nonlinear approach, radiation/diffraction forces are kept linear, but hydrostatic and Froude-Krylov actions are computed up to the instantaneous wetted surface, i.e., allowing for wave passage and motions nonlinear effects. In addition, the quadratic (nonlinear) roll damping contribution and mooring lines forces are considered.

6. CASE STUDY

A typical VLLC was used to analyze the different approaches for the roll damping prediction and their effects on roll responses. Table 1 presents the main particulars of the VLCC at a typical intermediate loading (draught) condition, while Figure 1 illustrates the 3D geometry of the hull and the mesh adopted in the numerical simulations.

Table 1: Main characteristics of the VLCC at the intermediate loading condition.

LBP	320.0	m
Breadth	54.5	m
Depth	27.8	m
Draught	14.7	m
Displacement	311 046	t
I_{44}	8.29E+07	t.m^2
GM	9.5	m

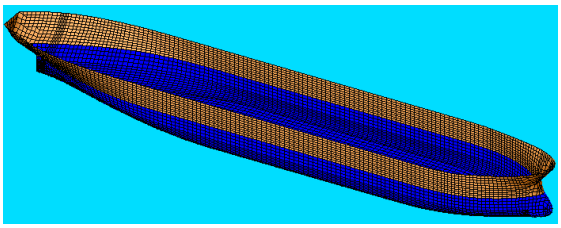

Figure 1: Panel geometry of the VLCC hull at the intermediate loading condition.

This hull has been tested in model scale (1:70) at the Brazilian Ocean Technology Laboratory (LabOceano) to assess its hydrodynamic behavior in waves as a Floating Production Storage and Offloading (FPSO) stationary unit, i.e., without forward speed, under wave conditions typical of Campos Basin, Brazil. The vessel was fitted with bilge keels of 1.00 m width and 127 m long, on both sides.

For the model tests, a simplified mooring system to restrain the horizontal motions was adopted. The simplified system only reproduced the horizontal (linear) restoring stiffness of the full system and consisted of four horizontal lines (two in the bow and tow in the stern).

Decay tests results

The decay tests have been performed for two initial angles, namely, 10º and 20º. The experimental series have been analyzed using the logarithmic and the decrement method. The roll resonant period was 14.4 s. Figures 2 and 3 illustrate the plots for the decay analyses of the 20º initial angle.

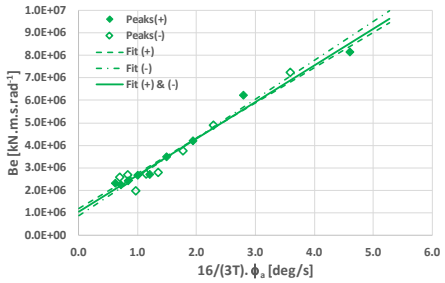

Figure 2: Equivalent roll damping from logarithmic decrement method.

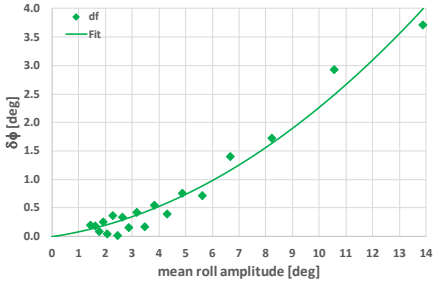

Figure 3: Curve of extinction of roll decay in Froude's method.

The roll damping coefficients from the decay tests of the 10º and 20º of initial angle are shown in Table 2.

Table 2: Roll damping coefficients from decay tests

Initial	Method	B_1 [kN.m.s.rad^{-1}]	B_2 [kN.m.s^2.rad^{-2}]
10º	Logarithmic	9.95E+05	9.63E+07
	Froude	1.61E+06	7.58E+07
20º	Logarithmic	1.01E+06	9.40E+07
	Froude	1.90E+06	7.52E+07

The results show significant differences among the coefficients obtained from both methods. For the linear coefficients, the differences were 62% and 88% for the 10º and 20º of initial roll, respectively. However, within a given method, there are not significant differences between the corresponding coefficients for 10º and 20º. Figures 4 and 5 present the time series of the experimental roll decay (Exp_PT15_302 and Exp_PT15_305) and the numerical simulations based on the uncouple roll motion equation with the roll damping coefficients

from the logarithmic decrement (Num_log10 and Numlog20) and the Froude methods (Num_Fr10 and Num_Fr20).

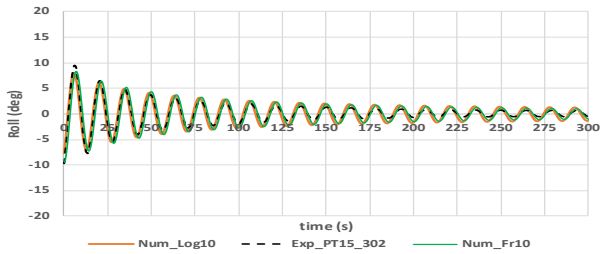

Figure 4: Time series of the roll decay for 10º initial angle.

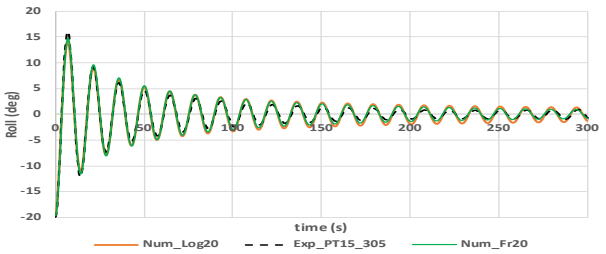

Figure 5: Time series of the roll decay for 20º initial angle.

Despite the significant differences in the roll damping coefficients between the logarithmic and Froude methods, the time series of the numerical simulations for both approaches agree satisfactorily with the experimental series. A slightly better agreement is observed for the Froude method, especially for the smaller roll motions.

Regular waves tests results

Based on the hybrid approach, for each test condition a single external roll damping coefficient has been estimated. A summary of the experimental roll response amplitudes (per meter of wave amplitude) in regular waves is shown in Fig. 6.

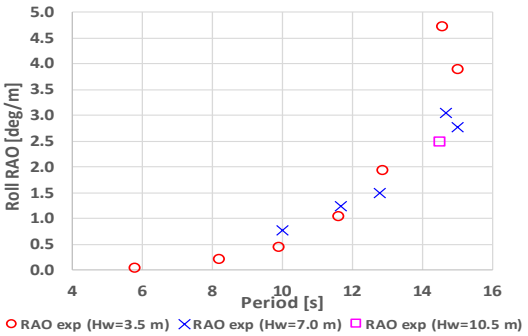

Figure 6: Experimental roll amplitudes for regular waves.

At the roll resonant period, different values were observed in the roll RAO with the increase of the incident wave height. Typically, this behavior is attributed to nonlinearities associated to hydrostatics and wave excitation loads. However, here, those differences will be assumed to be a consequence of different damping levels associated to the response amplitudes (or, implicitly, to the incident wave height. The set of external linear roll damping coefficients, i.e., additional to the potential damping, for the regular wave test conditions is presented in Figure 7 as a function of the incident wave period and height.

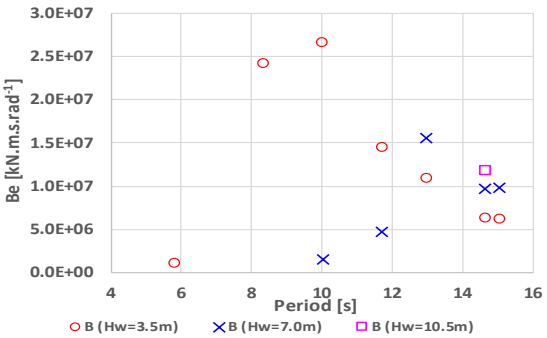

Figure 7: Roll damping coefficients for regular waves.

Some large variations along the wave period appeared in the estimation of the roll damping coefficients, particularly for periods 8 s and 10 s, however, those variations correspond to conditions where the roll responses displayed small amplitudes (less than 1 deg/m). Since the periods of those condition are far from the resonant roll period, the roll responses are almost insensitive to damping, so that exceptionally large values of damping coefficients were required to numerically calibrate those (small) responses. On the other hand, around the roll resonant period, where damping is an essential parameter, the various levels of roll damping associated to the incident wave height become evident. Except for the 13 s period, it is observed that the higher the wave height, the higher the roll damping coefficient.

Figure 8 presents the linearized roll damping coefficients around the roll resonant period from wave tests as function of the roll responses amplitude. For the sake of comparison, the experimental data from roll decay test at 20º of initial angle and Ikeda´s method predictions are also displayed.

In terms of equivalent linearized roll damping coefficients, the damping in waves is greater than in calm water (under roll decay), particularly for the larger responses. Unfortunately, since no tests were performed with smaller wave heights at the roll

resonant period, there is not enough data to verified that behavior for the smaller roll angles. However, if the fitting line of the wave test data is extrapolated to the smaller roll angles, the roll damping coefficients become closer or smaller than in roll decay.

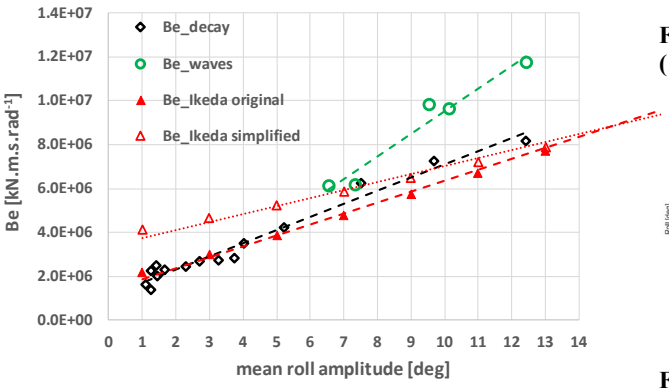

Figure 8: Linearized roll damping coefficients from decay tests, regular waves tests and Ikeda's original and simplified predictions for the resonant roll period.

To verify how those differences in the roll damping coefficients affect the predictions of roll motions, time domain numerical simulations of the wave tests conditions using the roll damping coefficients from both approaches (decay tests and regular waves) have been performed. Figs. 9 to 13 display the experimental roll and the corresponding simulations for some of the conditions around the roll resonance period and for different wave heights. The numerical simulations based on the calibrated damping coefficients from the roll responses in waves are Calib-Lin and Calib-NonLin, where the former refers to the linear model and the latter to the model with nonlinearities in hydrostatic and Froude-Krylov loads. The numerical simulations based on (linear + quadratic) roll decay coefficients are Decay-Lin and Decay-Nonlin. The latter also incorporates nonlinearities in hydrostatic and Froude-Krylov actions.

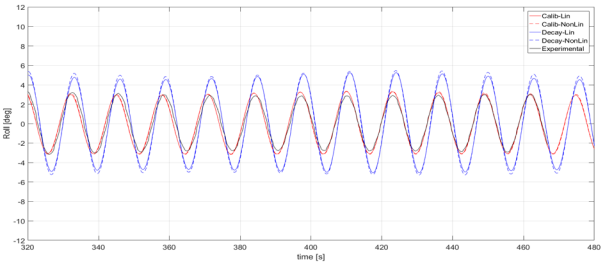

Figure 9: Roll from experiments and numerical simulations (T = 13.0 s, Hs = 2.9 m)

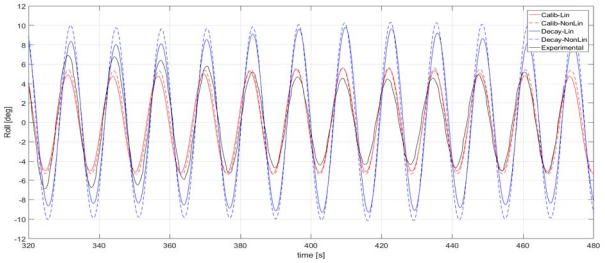

Figure 10: Roll from experiments and numerical simulations (T = 13.0 s, Hs = 6.4 m)

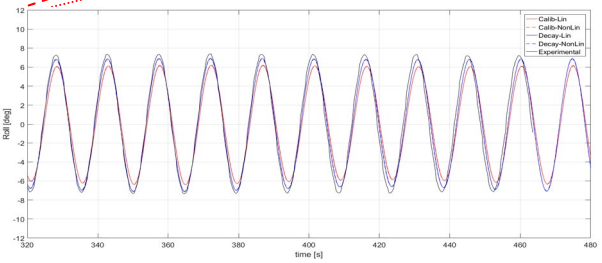

Figure 11: Roll from experiments and numerical simulations (T = 14.6 s, Hs = 3.2 m)

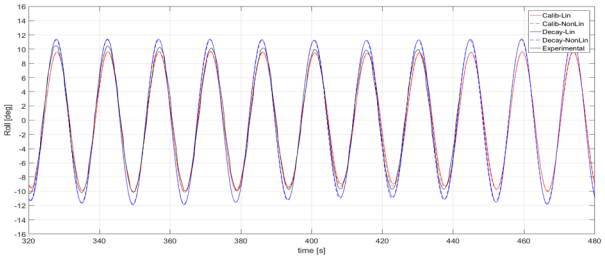

Figure 12: Roll from experiments and numerical simulations (T = 14.6 s, Hs = 6.8 m)

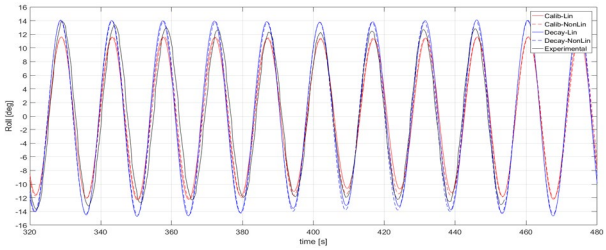

Figure 13: Roll from experiments and numerical simulations (T = 14.6 s, Hs = 9.8 m)

In general, the predictions based on roll decay damping coefficients overpredict the roll motions, while the approach based on wave responses, in average, presents a better agreement with the experimental results. It should be recalled that for the time series simulations, the time-domain model described in Section 5 have been used while for the roll damping coefficients estimation, the frequency domain model was adopted.

Regarding the nonlinearities in the hydrostatic and Froude-Krylov actions, it is evident that they are not relevant neither for the simulations based on roll decay coefficients nor for the ones based on the roll

response in waves. Therefore, at least, for the cases analyzed here, for a more realistic roll prediction, a more accurate prediction of roll damping in waves (even in its linearized form) seems to be more important than nonlinearities associated to restoring and Froude-Krylov.

Ikeda´s predictions

The two prediction approaches based on Ikeda´s method (the original and the simplified) have been implemented numerically and applied to the VLLC. The results from Ikeda´s prediction for the linearized damping at the roll resonant period are presented in Fig. 8. The original Ikeda's approach agrees quite well with the experimental roll decay data, especially for the smaller roll amplitudes, while the simplified Ikeda's approach overpredicts the roll decay damping coefficients for roll amplitudes below 10º. Compared to the damping coefficients from wave responses, both approaches based on Ikeda´s method display lower values. Thus, overestimation of roll responses in waves is expected if Ikeda´s damping coefficients are adopted.

Figures 14 and 15 present the components of the linearized roll damping coefficients from Ikeda's original and simplified approaches, respectively. The curve B_{Ikeda} represents the sum of the roll damping components, while the line *Fit* is the linear fitting to B_{Ikeda} curve for the estimation of coefficients B_1 and B_2. From the original Ikeda's method those values were 1.38E+06 kN.m.s/rad and 7.77E+07 kN.m.s^2/rad^2, respectively; while for the simplified approach the corresponding values were 3.38E+06 kN.m.s/rad and 5.68E+07 kN.m.s^2/rad^2, respectively. Those discrepancies can be attributed to significant differences in the estimations of wave damping (B_W) and bilge keel (B_{BK}) components between the two approaches.

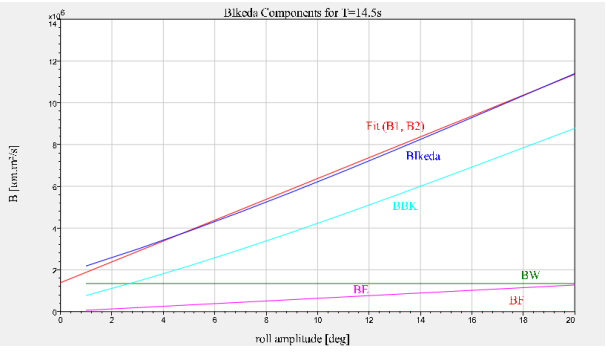

Figure 14: Roll damping components at roll resonant period from Ikeda's original method

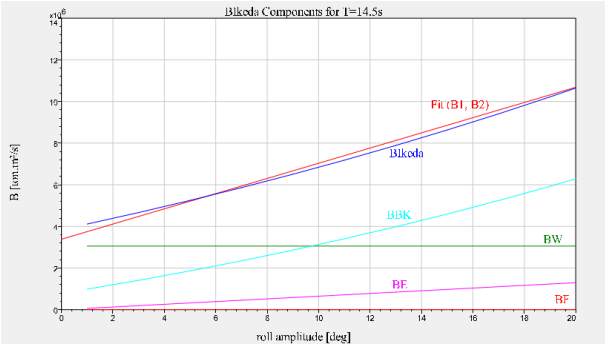

Figure 15: Roll damping components at roll resonant period from Ikeda's method simplified approach

Irregular waves tests results

For the model tests, three irregular sea conditions were specified for the VLCC: Irr1: 100-year extreme swell condition (JONSWAP spectrum: T_p=15.6 s, H_s=7.8 m, γ=1.7), Irr2: a one-year storm sea condition (JONSWAP T_p=8.6 s, H_s=4.5 m, γ=2.2) and Irr3: a Pierson-Moskowitz sea with T_p=17.8 s, H_s=5.9 m. γ represents the peak enhancement factor of the JONSWAP spectrum.

Based on the hybrid approach (following the frequency domain spectral expressions presented in Section 3), the spectrum of the numerical roll response was calibrated, and the corresponding external linearized damping coefficient was obtained for each test run. Then, time domain numerical simulations have been performed with the roll damping coefficients from roll decay tests and wave tests. The following approaches have been tested:

a) Three degree-of-freedom (3-DOF) model where only heave, roll and pitch motions have been considered.

b) Six-degree-of-freedom model with mooring lines and damping coefficients obtained from potential theory, except for the roll damping coefficient.

c) Six-degree-of-freedom model with mooring lines and damping coefficients considering linear viscous contributions in sway and/or yaw.

First, the direct assessment of roll motions used the linear hydrostatic and Froude-Krylov model; then, nonlinearities in those loads were introduced. Figures 16 to 18 present the roll response spectra from roll time series based on the linear model with the roll damping coefficient from wave tests. The comparison of the response spectra from the frequency domain

model (Num-FD) and from the experimental response spectra evidences the successful calibration of the roll damping coefficient for the three sea states.

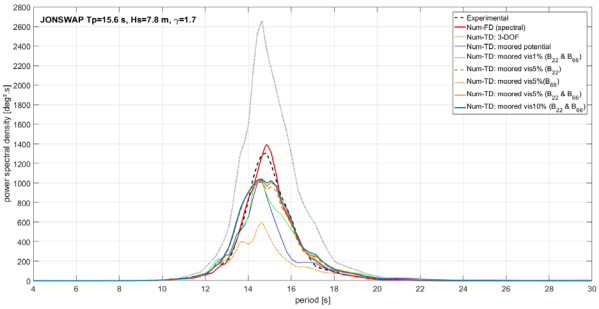

Figure 16: Roll response spectra for Irr1 - linear model with roll damping coefficients from wave tests.

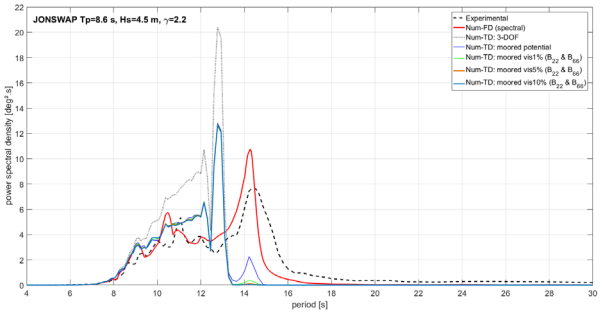

Figure 17: Roll response spectra for Irr2 - linear model with roll damping coefficients from wave tests.

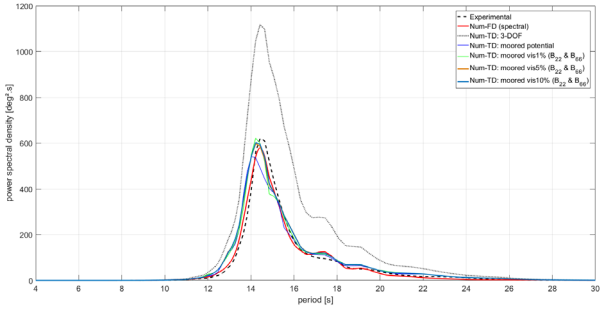

Figure 18: Roll response spectra for Irr3 - linear model with roll damping coefficients from wave tests.

Although a single roll damping coefficient has been calibrated for each sea state, the time domain numerical model (Num-TD) predicted significantly different roll motions. The 3-DOF, in which surge, sway and yaw motions were not allowed, substantially overpredicted the roll responses. More accurate predictions are obtained when the 6 DOFs are considered, which imply the inclusion of mooring line restoring effects. Furthermore, depending on the location of the peak of the sea spectrum, the quality of the predictions of the linear model can be substantially affected by the sway and yaw motions. For the sea condition Irr1 (whose peak period is around the roll resonance period), sway and yaw motions grow excessively (compared to the corresponding experimental responses) when only potential damping is considered for these DOFs. The overestimation of, especially, the sway motion causes the underestimation of roll response as observed in figure 16. To obtain better roll predictions, it was necessary to introduce linear external damping, at least, in the sway equation, to account for some viscous effects. In terms of critical damping, 1% of additional damping in sway and yaw greatly improved the predictions of roll. However, 5% and 10% of additional damping in those DOFs. display better predictions in all 6 DOFs. Figures 19 to 21 illustrate the experimental and numerical time series of sway (mean value has been removed), roll and yaw for sea state Irr1.

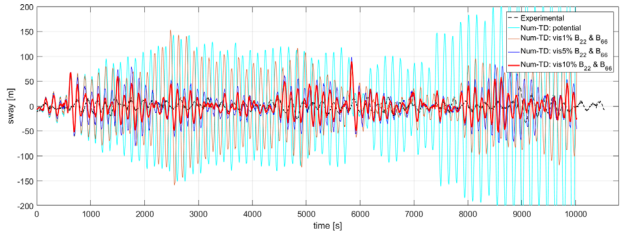

Figure 19: Sway responses for Irr1 - linear model with roll damping coefficients from wave tests.

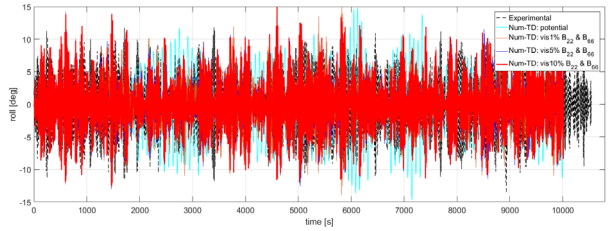

Figure 20: Roll responses for Irr1 - linear model with roll damping coefficients from wave tests.

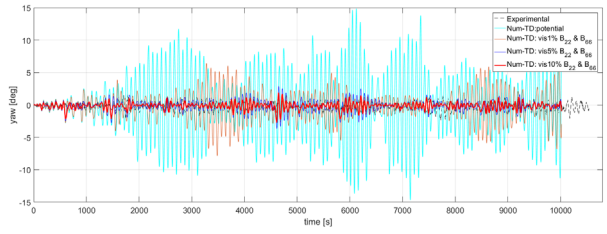

Figure 21: Yaw responses for Irr1 - linear model with roll damping coefficients from wave tests.

The time series of sway and yaw motions demonstrate that, at least, for the roll resonant sea state, the introduction of viscous effects (even in its linear form) in the sway and yaw dynamics has strong effect for the accurate predictions of motions. As the peak period of the sea state depart from the resonant roll period, the effect of additional (viscous) damping on sway and yaw motions

becomes less important, as evidenced in Figs. 17 and 18.

To assess the performance of the roll decay coefficients in irregular seas, time domain simulations in 6-DOFs have also been performed with the linear model (in terms of hydrostatic and Froude-Krylov actions), without the introduction of external damping on sway and yaw, i.e., only the linear plus quadratic roll damping coefficients have been allowed. Simulations with the nonlinear model (in terms of hydrostatic and Froude-Krylov actions) have also been performed for the cases with roll damping from wave tests (wave resp. NL) and from roll decay tests (decay NL). Figs. 22 to 24 present the roll response spectra of those simulations.

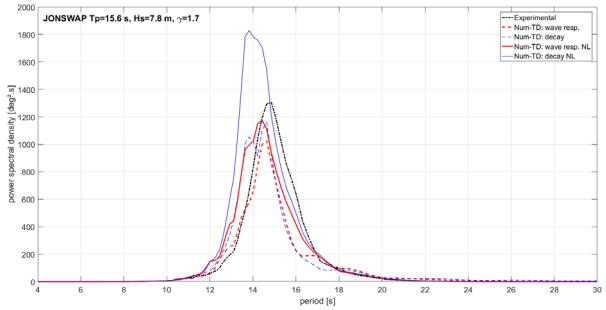

Figure 22: Roll response spectra for Irr1 – effect of roll decay damping coefficients and nonlinearities.

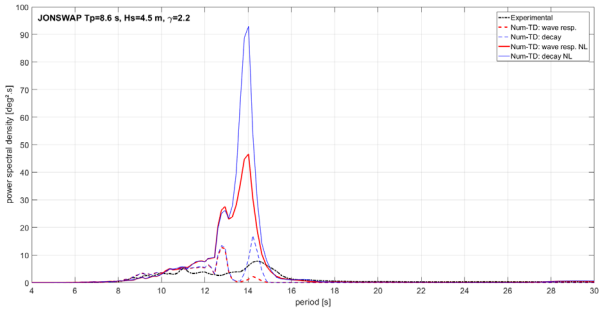

Figure 23: Roll response spectra for Irr2 – effect of roll decay damping coefficients and nonlinearities.

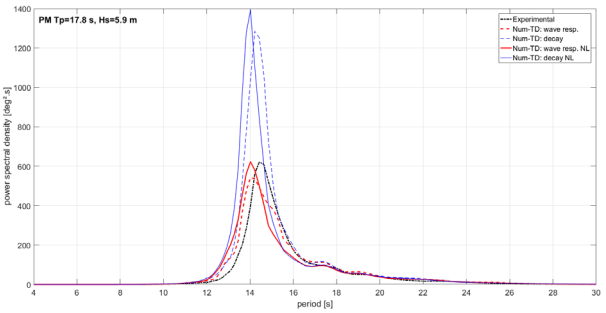

Figure 24: Roll response spectra for Irr3 – effect of roll decay damping coefficients and nonlinearities.

In general, the simulations based on roll decay damping coefficients predict larger roll responses than those of based on roll damping from the calibration of roll in waves, both for the linear and nonlinear model. The nonlinear model provided simulations with larger roll predictions than its linear counterparts, both considering the roll damping decay coefficients and the wave-response based coefficients.

The roll predictions for Irr2 seem to be not satisfactory in any of the time-domain approaches. It should be noticed, however, that under this sea condition the experimental measured roll was very small (barely exceeded 2º) and the frequency-domain (spectral) approach obtained after calibration of the external roll damping coefficient provided more satisfactory results (fig. 17). For Irr1, whose peak is close to the roll resonant period, except from the nonlinear model with decay coefficients, the results from all the time domain approaches presented satisfactory results, with slightly better agreement for the nonlinear model with damping coefficients from wave tests or the linear one with roll decay coefficients. For Irr3, it is quite evident that either the linear or nonlinear model can be adopted since the roll damping coefficient is calibrated from wave tests. Roll damping coefficients from decay tests excessively overpredict the roll responses for this sea state.

7. CONCLUSIONS

The present study analyzed the effect of roll damping on the direct assessment of roll motions for a VLLC without forward speed. Experimental data and numerical simulations have been explored or regular and irregular wave conditions. Three sources of roll damping coefficients have been applied: roll decay tests, calibration of experimental roll responses in waves and Ikeda's prediction method (the original and the simplified approach). The following conclusions can be summarized:

- The frequency domain model adopted for the estimation of the external linearized damping coefficients in regular and irregular waves was able to satisfactory calibrate the experimental roll responses.
- The linearized roll damping coefficients from the calibration of the experimental roll responses in waves displayed greater values than those from decay tests, especially for the larger roll amplitudes.

- Damping coefficients from original Ikeda's method displayed particularly good agreement with decay test results. Yet, the simplified Ikeda's approach overpredicted roll damping for the smaller roll amplitudes and underpredicted for the larger ones. Wave and bilge keel damping components have been regarded as the main source of discrepancies.
- Roll damping coefficients from decay tests tend to overpredict the roll responses.
- The effect of nonlinearities in hydrostatic and Froude-Krylov actions are not relevant for the regular wave conditions, while for irregular waves the influence is more apparent. In general, those nonlinearities tend to produce larger responses than their linear counterparts.
- Sway and yaw motions are essential for accurate time-domain roll motion predictions. 3-DOF models (heave, roll, and pitch) excessively overpredict roll responses.
- For the sea states with peak periods around roll resonance, the introduction of external (viscous) linearized damping on sway and yaw motions improve the prediction of roll responses.
- Accurate estimation of roll damping for each test condition is more relevant than the effect of nonlinearities in restoring and Froude-Krylov actions. Thus, roll predictions based on (linearized) roll damping coefficients from wave tests are, in general, more reliable than those based on roll decay coefficients.

ACKNOWLEDGEMENTS

This work was developed in the context of a research cooperation project among LabOceano-UFRJ, CENPES-Petrobras and Tecgraf-PUC/RJ. The Authors acknowledge the financial support from the Special Participation Funds for Research and Development of the National Agency of Petroleum, Natural Gas and Biofuels (ANP), Brazil.

REFERENCES

Bačkalov, I., Bulian, G., Cichowicz, J., et al., 2016. Ship stability, dynamics and safety: Status and perspectives from a review of recent STAB conferences and ISSW events. Ocean Engineering 116, 312-349.

Hashimoto, H., Omura, T., Matsuda, A., et al., 2019. Several remarks on EFD and CFD for ship roll decay. Ocean Engineering 186, 106082.

Himeno, Y., 1981. Prediction of Ship Roll Damping - State of the Art. Dept. of Naval Architecture and Marine Engineering. The University of Michigan.

Ikeda, Y., 2018. Historic Review of Ikeda's Prediction Method for Ship Roll Damping and its Future, 13th International Conference on Stability of Ships and Ocean Vehicles (STAB 2018), Kobe, Japan, pp. 6-15.

Kawahara, Y., Maekawa, K., Ikeda, Y., 2012. A simple prediction formula of roll damping of conventional cargo ships on the basis of Ikeda's method and its limitation. Journal of Shipping and Ocean Engineering 2 (4), 201.

Manderbacka, T., Themelis, N., Bačkalov, I., et al., 2019. An overview of the current research on stability of ships and ocean vehicles: The STAB2018 perspective. Ocean Engineering 186, 106090.

Oliva-Remola, A., Pérez-Rojas, L., 2019. A step forward towards developing an uncertainty analysis procedure for roll decay tests, 17th International Ship Stability Workshop, Helsinki, Finland, pp. 289-296.

Oliva-Remola, A., Pérez-Rojas, L., Díaz-Ojeda, H.R., 2018. Ship Roll Damping Estimation: A Comparative Study of Different Roll Decay Tests, 13th International Conference on Stability of Ships and Ocean Vehicles, Kobe, Japan, pp. 312-322.

Oliveira, M.C.d., de Barros Mendes Kassar, B., Gomes Coelho, L.C., et al., 2019. Empirical and experimental roll damping estimates for an oil tanker in the context of the 2nd generation intact stability criteria. Ocean Engineering 189, 106291.

Rodríguez, C.A., Esperança, P.T.T., Oliveira, M.C., 2019. Estimation of Roll Damping Coefficients Based on Model Tests Responses of a FPSO in Waves, ASME 2019 38th International Conference on Ocean, Offshore and Arctic Engineering.

Smith, T., 2018. Determination of Roll Damping for Empirical Measurements, 13th International Conference on Stability of Ships and Ocean Vehicles, Kobe, Japan, pp. 301-311.

Spouge, J.R., 1988. Non-linear analysis of large-amplitude rolling experiments. International Shipbuilding Progress 35 (403), 271-320.

Wassermann, S., Sumislawski, P., Moustafa, A., 2018. Accelerated HERM Technique by Induced Artificial Damping for Efficient Ship Roll Damping Estimation, 13th International Conference on Stability of Ships and Ocean Vehicles, Kobe, Japan, pp. 331-338.